



## Active Vibration Control of a Nonlinear System with Optimizing The Controller Coefficients Using Metaheuristic Algorithms

M. AbdolMohammadi<sup>1</sup>, H. Ahmadi<sup>1</sup>, S. M. Varedi-Koulaei<sup>1\*</sup>, J. Ghalibafan<sup>2</sup>

<sup>1</sup> Department of Mechanical and Mechatronics Engineering, Shahrood University of Technology, Shahrood, Iran.

<sup>2</sup> Department of Electrical and Robotics Engineering, Shahrood University of Technology, Shahrood, Iran.

**ABSTRACT:** An active vibration absorber is utilized in this study for a nonlinear system with unknown multi-harmonic frequency disturbance. At first, a function for disturbance force and its first and second derivatives are estimated. Then the position of the main system is controlled by feedback linearization and sliding mode controllers. A magnetic actuator is designed, which is controlled by a sub-controller. Liunberger observer estimates disturbance function, and the feedback linearization and sliding mode controllers regulate the main system's position. Metaheuristic algorithms obtain the controller's coefficients to minimize settling time and errors. Four different techniques, namely, Genetic algorithm, Particle swarm optimization, Simulated annealing, and Teaching-learning-based optimization, are utilized for the optimization process. A magnetic actuator is designed using Faraday and Lorentz's law for applying the controlling force to the system. Simulation results of the observer have been compared to real value, and the results show the excellent effect of active vibration absorbers on vibration suppression. Moreover, optimizing the controller coefficient shows an improvement in settling time and error. Comparing the algorithms, particle swarm optimization has the best cost function, where Teaching-learning-based optimization has the best-averaged results.

### Review History:

Received: Mar. 12, 2021

Revised: May, 25, 2021

Accepted: Jul. 17, 2021

Available Online: Jul. 19, 2021

### Keywords:

Active vibration absorber

Sliding mode control

Liunberger

Metaheuristic optimization algorithms

Magnetic actuator

### 1- Introduction

Nowadays, vibrations are attractive and more applicable. Vibration is intentionally used in some systems, like the vibratory bowl for automatic feeding, operator interface in phones, gaming instruments, etc. In some systems, the goal is vibration suppression. In this case, a vibration absorber can be used. In general, vibration absorbers can be divided into two main categories: passive vibration absorbers and active vibration absorbers. Passive vibration absorbers are reduced oscillations without control strategy and actuators. But in active vibration absorbers, oscillations are reduced using a control method in different frequencies.

Vibration absorbers are used in high structures, bridges, towers, high voltage cables, etc. Also, vibration absorbers are used in rotary systems to prevent the torsion axis. The advantage of using active vibration absorbers is to minimize the size of the actuators. For example, a bridge to prevent vibration without an absorber needs to use a huge actuator. Still, when it uses an active vibration absorber, the actuator can be very small. For different applications of vibration absorbers, exist several types of actuators. In bridges and building applications, hydraulic actuators have been used, and magnetic or electrical actuators can be used in smaller applications.

Since 1928, the regulation of vibrating absorbing has

begun by Armstrong and Dan Hatg, and has progressed so far, and its applications have expanded [1]. Until the last decade, most efforts were made to use passive vibration absorber in various applications [2-5], and scientists looked at how vibration absorber was used and responsive. For example, the vibration absorber in bridges is studied by Chen and Kareem [6] in 2003. The use of a vibration absorber combined with other methods of reducing vibrations, for example, vibration isolation, provides the basis for other work in this field [4, 5]. In the following, with the combination of vibration absorbers with control systems, an active vibration absorber appeared. An active vibration absorber has much more power than a passive vibration absorber. Active vibration absorber has a more frequency range for control [7-10]. Various control methods are used in active vibration absorbers. Each of these methods has particular advantages in reducing vibrations. These control methods are also performed on the beams. Bailly and Hubbard [11] (1985) controlled the vibrations of the beam by using piezoelectric sensors and actuators for a cantilever beam. The combination of a vibration absorber with control is not enough when the disturbance is in the system. The disturbance estimation can be helpful in systems control and vibration reduction. Also, an observer can help to estimate the system states in control. Mirowich used the Liunberger observer in 1985 to estimate the system states. Estimators not only gives system states but also can estimate disturbance [7, 10, 12, 13]. Oscillation control is one of the important

\*Corresponding author's email: varedi@shahroodut.ac.ir



tasks of an active vibration absorber. Due to high frequency or unknown disturbance in uncertain vibration systems, using robust controllers is necessary. The sliding mode controller is the most straightforward and most applicable control strategy for uncertain systems [14-17]. Optimizing the coefficients of the controllers leads the system to the desired position. The integrated control and structure design optimization problem have been investigated from a response to the disturbance point of view is presented by McLaren and Slater in 1993. The output feedback controllers were employed in the control strategy, and quantitate results were presented [18]. Integrated control and structural optimization design model for piezoelectric intelligent truss structures have been presented. In Zhao et al.'s [19] study in 2009, the feedback gain is optimized. Zhang et al. [20] in 2017 propose a method for topology optimization of piezoelectric laminated plates for minimizing the energy consumption with active vibration control under harmonic excitation. Some more study in vibration optimization problems is about designing a passive vibration absorber and tuning the mass, spring, and damper [21-23].

The magnetic actuator has several types and is also used in many different fields. In 2000, Howe presented the applications of various types of magnetic actuators in aviation systems [24]. Linear magnetic actuators are more complex than rotational magnetic actuators. Magnetic actuators are used in a variety of applications. A simple type of linear magnetic actuator is to form magnet arrays [25, 26]. This structure is nonlinear, and researchers use different methods to improve this actuator to reduce nonlinear effects. Clarke et al., in 1995, tried to linearize this type of actuator. Linear magnetic actuators are usually presented in innovative ways. For example, Kim et al. [29] In 2005 and Li et al. [28] ] in 2007 presented a very similar actuator that is very effective in short course motion. These types of actuators with small moves are used in the automatic valves, and due to the high nonlinearity nature of these valves, scientists try to control these valves using different control [30]. Researches on linear magnetic actuators are still ongoing, and various ideas for these actuators are presented. For example, in 2009, Lierop et al. [31] presented a planar magnetic actuator. In micro dimensions, using a magnetic actuator is common because these actuators have a very high ability in micro dimensions and are more capable of controlling in this field. A study in 1996 also showed that magnetic actuators, in the micro dimensions, could be used simultaneously as position sensors [32]. The combination of active vibration absorbers and magnetic actuators can control the vibration systems in the presence of disturbance.

Optimization of the controller's coefficient based on minimizing the settling time is the current study's goal. To this end, the modeling of these systems is presented, and the estimator of disturbance is designed. Then, the effects of controller coefficients on feedback linearization and the sliding mode controllers are investigated, and their optimal values are selected using four metaheuristic algorithms. Finally, the simulation results are presented for the optimal

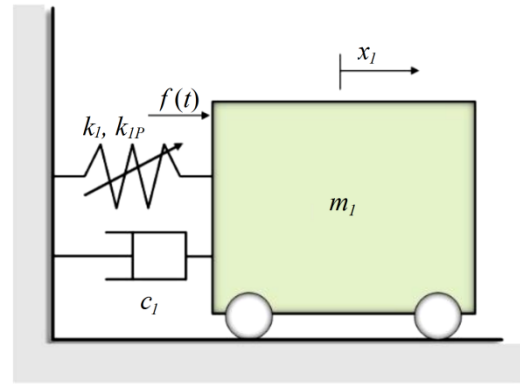


Fig. 1. Primary system

designs of the controller.

## 2- Modeling

### 2- 1- Mechanical system modeling

To control a vibration system similar to Fig. 1, an active vibration absorber is used, according to Fig. 2. In the presented system, the control force  $u$  is applied to the absorber by a magnetic actuator. In this system, the system consists of a mass and linear damper and a nonlinear spring that it's vibrated by the unknown multi-harmonic force  $f(t)$  that is joined to a vibration absorber by a linear spring.

Fig. 1 shows the primary system in which vibrations are transmitted by a linear spring to the vibration absorber, and the damper in the absorber system is joined to the earth. The characteristic of nonlinear spring in primary mass as shown in Eq. (1), where  $x_1$  is the main mass position,  $k_1$  is the linear stiffness coefficient of the spring and  $k_{1p}$  is the nonlinear stiffness coefficient of spring, which is in the condition  $x_1 = 0$  the spring is in the primary length.

$$P(x_1) = k_1 x_1 + k_{1p} x_1^3 \quad (1)$$

Using Newton's second law for the primary and absorber systems, one can obtain two second-order differential equations for primary and absorber systems. According to Fig. 2, the mechanical equations are obtained follow as:

$$m_1 \ddot{x}_1 + c_1 \dot{x}_1 + k_1 x_1 + k_{1p} x_1^3 - k_2 (x_2 - x_1) = f(t) \quad (2)$$

$$m_2 \ddot{x}_2 + c_2 \dot{x}_2 + k_2 (x_2 - x_1) = u(t) \quad (3)$$

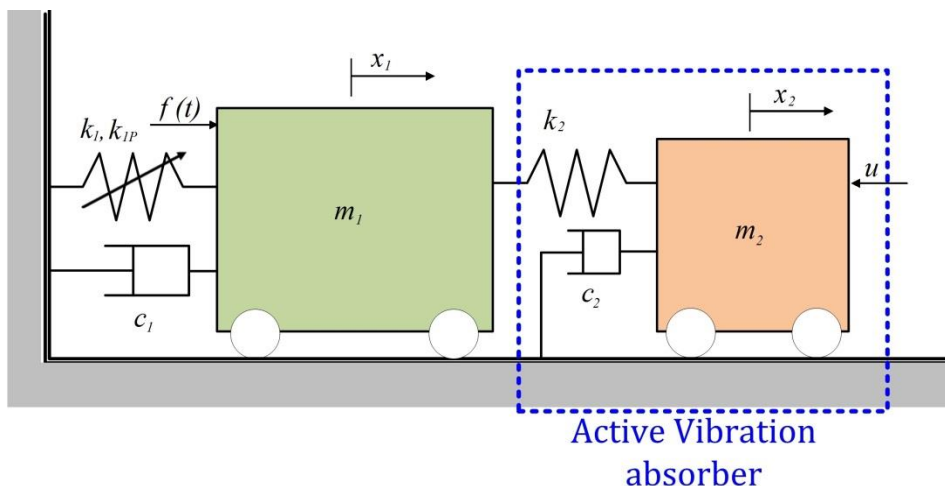


Fig. 2. Primary system and active vibration absorber

In Eq. (2),  $x_1$  is the main mass position and  $x_2$  is the position of the absorber mass, which is equal to zero in the primary length. To obtain the state space equations, the primary mass position is defined as  $z_1 = x_1$ , and the absorber mass position is defined as  $z_3 = x_2$ . Then, with the definition of  $z_2$  and  $z_4$  as respectively, the primary and absorber mass velocity is obtained in state space. So, by inserting  $x_1 = z_1$  and  $x_2 = z_3$  and  $\dot{x}_1 = z_2$  and  $\dot{x}_2 = z_4$ , the space-state equations are obtained:

$$\begin{aligned} \dot{z}_1 &= z_2 \\ \dot{z}_2 &= -\frac{(k_1 + k_2)}{m_1} z_1 - \frac{k_{1P}}{m_1} z_1^3 - \frac{c_1}{m_1} z_2 + \frac{k_2}{m_1} z_3 + \frac{1}{m_1} f(t) \end{aligned} \quad (4)$$

$$\begin{aligned} \dot{z}_3 &= z_4 \\ \dot{z}_4 &= \frac{k_2}{m_2} z_1 - \frac{c_2}{m_2} z_4 - \frac{k_2}{m_2} z_3 + \frac{1}{m_2} u \end{aligned}$$

### 2- 2- Electrical system modeling

The electrical system consists of the coil of a magnetic actuator and a current-carrying wire. Fig. 3 generally shows the actuator.

Concerning Fig. 3, two coils are located near together. The magnetic core inside each of the coils increases the intensity of the magnetic field and provides an appropriate direction

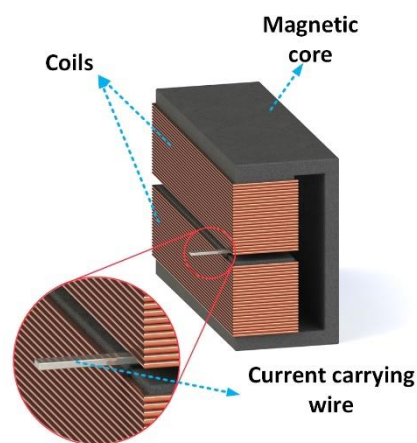


Fig. 3. generally structure of an actuator

for the magnetic field to prevent loss of the field. The current-carrying wire is in a uniform field. The wire is passed from the magnetic field. According to the Lorentz law, it is created a force on the wire and the force will be applied to the absorber. The modeling of the magnetic actuator generally consists of two parts. The first part is calculating the force generated in the current-carrying wire that depends on the value of current and the intensity of the magnetic field. The second part is the circuit modeling of the actuator, which consists of an electric circuit with voltage input and a current output that produces the desired force according to the first part.

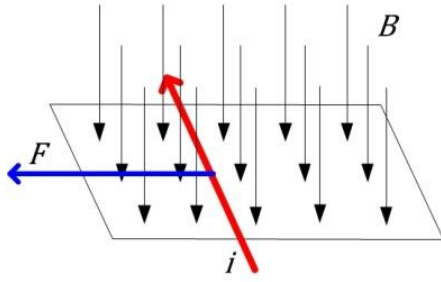


Fig. 4. Modeling of the actuator

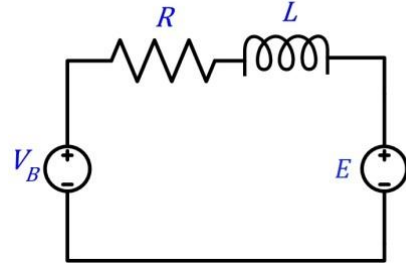


Fig. 5. The equivalent circuit of the actuator

### 2- 2- 1- Calculation of the force generated in the actuator

The applied force to the electrical charge is presented in Eq. (5) [33].

$$F_m = qV_e \times B \quad (5)$$

where  $q$  is the electrical charge and  $V_e$  is the velocity of the electrical charge, and  $B$  is the density of magnetic field intensity. In general, Eq. (5) means that if an electrical charge moves in the magnetic field with velocity  $V_e$ , then the force  $F_m$  is applied to it. The differential form of Eq. (5), that is the applied force on  $dl$ , can be written as Eq. (6).

$$dF_m = -N_e eS |dl| V_e \times B = -N_e eS |V_e| dl \times B \quad (6)$$

where  $dl$  is a small element of a conductor with section cross  $S$ ,  $N_e$  is the number of electrons per unit volume, and  $e$  is the electron charge. In Eq. (6), the value of  $N_e eS |V_e|$  is equal to the amount of current which passes from the conductor, so we can write:

$$dF_m = I dl \times B \quad (7)$$

Eq. (7) is called the Lorentz law. This law shows that if a current-carrying conductor is perpendicular to the magnetic field, then the force  $F_m$  is applied to it. Fig. 4 shows how the actuator applies the force. This law is in a static situation, and when the wire moves in the field, voltage is induced in the wires which reduces the current in the wire, so the force is generated and absorbs energy from the system. The absorbed energy is seen in inducted voltage. The induced voltage can be obtained from Faraday's law. Faraday's law illustrates if a wire moves with velocity  $V_e$  in a magnetic field, then the

voltage  $E$  is induced. Eq. (8) calculates the value of the voltage induced in the wire with the length  $L_w$  [33].

$$E = (V_e \times B) L_w \quad (8)$$

### 2- 2- 2- Actuator electrical circuit modeling

The equivalent circuit of the system is shown in Fig. 5, where  $V_B$  is the input voltage of the wire, and  $R_e$  is the total resistance of the circuit, and  $E$  is the voltage induced in the wire, and  $L$  is the self-inductance of the wire.

The relation between current and input voltage is obtained using Kirchhoff's law according to Fig. 5.

$$V_B - R_e i - E - L \frac{di}{dt} = 0 \quad (9)$$

Eq. (9) is a first-order differential equation.  $V_B$  is input voltage as the input of the electric system, and the current is a state variable. The state-space equations of the electrical system are obtained in Eq. (10).

$$\frac{di}{dt} = \frac{-R_e i}{L} - \frac{E}{L} + \frac{1}{L} V_B(t) \quad (10)$$

### 2- 2- 3- Calculation of the coils magnetic field intensity

In Eqs. (7) and (8), the value  $B$  represents the density of the magnetic field in the coils. Fig. 6 shows a rectangular loop of the coil. For each part of the wire, the field in the center of the rectangular is computed and then the summation of these fields is the coil field for one loop.

To calculate the field at a distance  $r$  for a wire with

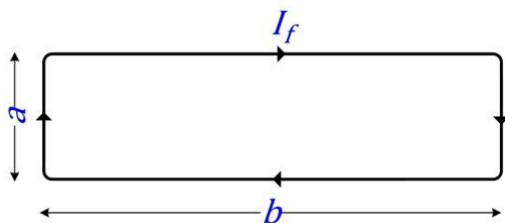


Fig. 6. One ring of the coil

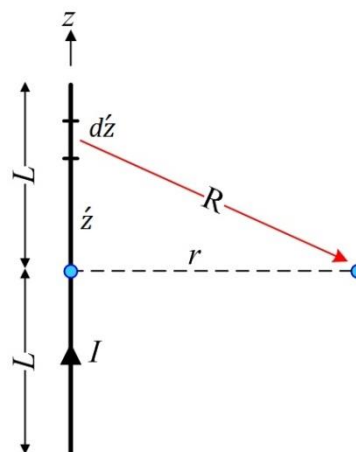


Fig. 7. Calculation of magnetic field a wire with length  $2L$  [33]

length  $2L$  as shown in Fig. 7, first, the magnetic potential is obtained. The cylindrical coordinates  $(a_r, a_\varphi, a_z)$  are used to calculate the magnetic potential.

$$A = \hat{a}_z \frac{\mu_0 I}{4\pi} \ln \frac{\sqrt{L^2 + r^2} + L}{\sqrt{L^2 + r^2} - L} \quad (11)$$

The density of the magnetic field is obtained with regard to the magnetic potential as Eq. (12) [33].

$$B = \nabla \times A \quad (12)$$

$$B = \nabla \times (\hat{a}_z A) = \hat{a}_r \frac{1}{r} \frac{\partial A}{\partial \varphi} - \hat{a}_\varphi \frac{\partial A}{\partial r} \quad (13)$$

The value of  $\partial A / \partial \varphi$  is zero because the magnetic potential is constant at a specific distance from the wire so that we can write:

$$B = \hat{a}_\varphi \frac{\mu_0 I L}{2\pi r \sqrt{L^2 + r^2}} \quad (14)$$

Eq. (14) shows the field around a wire with length  $2L$  in distance  $r$ .

According to Fig. 6, the field generated by the rectangle's length in its center is obtained as

$$B = \frac{4N \mu I_f \sqrt{a^2 + b^2}}{\pi(ab)} \quad (15)$$

Finally; Magnetic force can be obtained according to

the magnetic field by Eqs. (15) and (10). The wire's self-inductance can be considered zero due to the short length of the wire and its single ring. The mutual inductance between the coil and the wire is also very small for three reasons: the current in the coil is constant, the field created by the wire is very small, and the magnetic cores in the coils. So the Eq. (9) can be expressed as

$$i = \frac{V_B - E}{R_e} \quad (16)$$

According to Eq. (7), we can write:

$$F_m = ia \times B \quad (17)$$

Using Eqs. (8), (16), and (17), the magnetic force is obtained as follows.

$$F_m = \frac{a}{R_e} B (V_B - aBV_e) \quad (18)$$

Substituting Eq. (15) into Eq. (18), Eq. (19) is obtained:

$$F_m = \frac{4\mu N I_f \sqrt{a^2 + b^2}}{R_e b \pi} \times \left( V_B - \frac{4\mu N I_f V_e \sqrt{a^2 + b^2}}{b \pi} \right) \quad (19)$$

Eq. (19) shows the magnitude of the force generated by the magnetic actuator which the input voltage can control  $V_B$

### 3- Control

A nonlinear control strategy is different based on the model uncertainty of the system. When a nonlinear system is completely known and certain, the feedback linearization control method is the simplest control method that achieves the desired response. Derivation of accurate model equations is impossible; therefore, the feedback linearization method is not suitable for these systems. There are several methods to compensate for uncertainties. One of the control methods for a nonlinear system, including the uncertainty, is the sliding mode control method, which guarantees the system's stability because the sliding mode controller is obtained based on the Lyapunov stability theory.

In this study, to control the mass-spring-damper system with a vibration absorber, feedback linearization and sliding mode control methods are used. These methods require the estimation of the disturbance imposed on the system. The disturbance is unknown but it is harmonic. Because the estimator's speed and accuracy are essential, the Liunberger observer estimates the disturbance force. Actually, the Liunberger estimator using the input and output of the actual system calculate the disturbance force on the system, which is explained in detail in the next section.

#### 3- 1- Disturbance force estimator

As mentioned above, to control the mass-spring-damper system with a vibration absorber, an appropriate estimation of the disturbance force is first required. The disturbance force is the summation of several harmonic forces with different amplitudes and frequencies. The disturbance is applied to the main mass, according to Fig. 2. The goal of control is so that  $y = z_1$  tracks the desired value, to this end, we must differentiate from the state space equations such that  $u$  appears in the output dynamics as Eq. (20).

$$\begin{aligned}
 y &= z_1 \\
 \dot{y} &= z_2 \\
 \ddot{y} &= -\left(\frac{k_1+k_2}{m_1}\right)y - \frac{k_{1p}}{m_1}y^3 - \frac{c_1}{m_1}\dot{y} + \frac{k_2}{m_1}z_3 + \frac{1}{m_1}f(t) \\
 y^{(3)} &= -\left(\frac{k_1+k_2}{m_1}\right)\dot{y} - 3\frac{k_{1p}}{m_1}y^2\dot{y} - \frac{c_1}{m_1}\ddot{y} + \frac{k_2}{m_1}z_4 + \frac{1}{m_1}\dot{f}(t) \\
 y^{(4)} &= \frac{k_2^2}{m_1m_2}y - \left(\frac{k_1+k_2}{m_1}\right)\ddot{y} -
 \end{aligned} \tag{20}$$

$$\begin{aligned}
 &3\frac{k_{1p}}{m_1}y^2\ddot{y} - 6\frac{k_{1p}}{m_1}y\dot{y}^2 - \frac{c_1}{m_1}y^{(3)} \\
 &- \frac{k_2^2}{m_1m_2}z_3 - \frac{k_2c_2}{m_1m_2}z_4 + \frac{k_2}{m_1m_2}u + \frac{1}{m_1}\dot{f}(t)
 \end{aligned}$$

According to Eq. (20), we can obtain the state variables in terms of output and its derivatives, derived as Eq. (21).

$$\begin{aligned}
 z_1 &= y \\
 z_2 &= \dot{y} \\
 z_3 &= \frac{m_1}{k_2}\ddot{y} + \frac{c_1}{k_2}\dot{y} + \frac{k_1+k_2}{k_2}y + \frac{k_{1p}}{k_2}y^3 - \frac{1}{k_2}f(t) \\
 z_4 &= \frac{m_1}{k_2}y^{(3)} + \frac{c_1}{k_2}\ddot{y} + \frac{k_1+k_2}{k_2}\dot{y} + 3\frac{k_{1p}}{k_2}y^2\dot{y} - \frac{1}{k_2}\dot{f}(t)
 \end{aligned} \tag{21}$$

Now, substituting Eq. (21) into Eq. (20),  $y^{(4)}$  is obtained as Eq. (22).

$$\begin{aligned}
 y^{(4)} &= -\left(\frac{c_1}{m_1} + \frac{c_2}{m_2}\right)y^{(3)} - \left(\frac{k_1+k_2}{m_1} + \frac{k_2}{m_2} + \frac{c_1c_2}{m_1m_2}\right)\ddot{y} - \left[\frac{c_2k_2}{m_1m_2} + \frac{c_2(k_1+k_2)}{m_1m_2}\right]\dot{y} - \frac{k_1k_2}{m_1m_2}y - \frac{k_2k_{1p}}{m_1m_2}y^3 - 3\frac{k_{1p}}{m_1}y^2\ddot{y} - 6\frac{k_{1p}}{m_1}y\dot{y}^2 - 3\frac{c_2k_{1p}}{m_1m_2}y^2\dot{y} + \frac{k_2}{m_1m_1}u(t) + \xi(t)
 \end{aligned} \tag{22}$$

where

$$\xi(t) = \frac{k_2}{m_1m_2}f(t) + \frac{c_2}{m_1m_2}\dot{f}(t) + \frac{1}{m_1}\ddot{f}(t) \tag{23}$$

In fact, Eq. (23) is the new disturbance function required for control, which should be estimated. Indeed, the  $\xi$  function is estimated to control the system instead of  $f(t)$ .

Liunberger observer is used to estimating the function  $\xi$ , which uses the Taylor series prediction signal as Eq. (24) [10].

$$\xi(t) = \sum_{i=0}^{r-1} p_i t^i \tag{24}$$

where all  $p_i$  coefficients are unknown and  $t$  is the time variable of the series. The degree of Eq. (25) indicates the order of the observer. The accuracy of prediction and processing is increased by increasing the order of the observer.

$$\begin{aligned} \dot{\xi}_1 &= \xi_2 \\ \dot{\xi}_2 &= \xi_3 \\ &\vdots \\ \dot{\xi}_{r-1} &= \xi_r \\ \dot{\xi}_r &= 0 \end{aligned} \tag{25}$$

where  $\xi_1 = \xi$ ,  $\xi_2 = \dot{\xi}$ , ..., and  $\xi_r = \xi^{(r-1)}$ .

Concerning Eqs. (22) and (25), and by defining  $y = \eta_1 = z_1$  and  $\dot{y} = \eta_2, \dots$ , the developed model of the predictive signal of the dynamical system is as follows.

$$\begin{aligned} \dot{\eta}_1 &= \eta_2 \\ \dot{\eta}_2 &= \eta_3 \\ \dot{\eta}_3 &= \eta_4 \\ \dot{\eta}_4 &= -\left(\frac{c_1}{m_1} + \frac{c_2}{m_2}\right)\eta_4 - \\ &\left(\frac{k_1+k_2}{m_1} + \frac{k_2}{m_2} + \frac{c_1c_2}{m_1m_2}\right)\eta_3 - \\ &\left[\frac{c_2k_2}{m_1m_2} + \frac{c_2(k_1+k_2)}{m_1m_2}\right]\eta_2 - \\ &\frac{k_1k_2}{m_1m_2}\eta_1 - \frac{k_2k_{1p}}{m_1m_2}\eta_1^3 - 3\frac{k_{1p}}{m_1}\eta_1^2\eta_3 - \\ &6\frac{k_{1p}}{m_1}\eta_1\eta_2^2 - 3\frac{c_2k_{1p}}{m_1m_2}\eta_1^2\eta_2 + \frac{k_2}{m_1m_1}u(t) + \xi_1 \end{aligned} \tag{26}$$

$$\begin{aligned} \dot{\xi}_1 &= \xi_2 \\ \dot{\xi}_2 &= \xi_3 \\ &\vdots \\ \dot{\xi}_{r-1} &= \xi_r \\ \dot{\xi}_r &= 0 \end{aligned}$$

According to Eq. (26), we can make the Liunberger observer as Eq. (27). We can determine the estimator poles by choosing the appropriate values of  $\beta_0 \dots \beta_r$ .

$$\begin{aligned} \dot{\eta}_1 &= \hat{\eta}_2 + \beta_7(y - \hat{y}) \\ \dot{\eta}_2 &= \hat{\eta}_3 + \beta_6(y - \hat{y}) \\ \dot{\eta}_3 &= \hat{\eta}_4 + \beta_5(y - \hat{y}) \\ \dot{\eta}_4 &= -\left(\frac{c_1}{m_1} + \frac{c_2}{m_2}\right)\eta_4 - \\ &\left(\frac{k_1+k_2}{m_1} + \frac{k_2}{m_2} + \frac{c_1c_2}{m_1m_2}\right)\eta_3 - \\ &\left[\frac{c_2k_2}{m_1m_2} + \frac{c_2(k_1+k_2)}{m_1m_2}\right]\eta_2 - \\ &\frac{k_1k_2}{m_1m_2}\eta_1 - \frac{k_2k_{1p}}{m_1m_2}\eta_1^3 - 3\frac{k_{1p}}{m_1}\eta_1^2\eta_3 - \\ &6\frac{k_{1p}}{m_1}\eta_1\eta_2^2 - 3\frac{c_2k_{1p}}{m_1m_2}\eta_1^2\eta_2 + \\ &\frac{k_2}{m_1m_1}u(t) + \hat{\xi}_1 + \beta_4(y - \hat{y}) \\ \widehat{\xi}_1 &= \hat{\xi}_2 + \beta_3(y - \hat{y}) \\ \widehat{\xi}_2 &= \hat{\xi}_3 + \beta_2(y - \hat{y}) \\ \widehat{\xi}_3 &= \hat{\xi}_4 + \beta_1(y - \hat{y}) \\ \widehat{\xi}_4 &= \beta_0(y - \hat{y}) \end{aligned} \tag{27}$$

### 3- 2- Active vibration absorber

From the control point of view, vibration absorbers are divided into two groups: 1- active vibration absorbers 2- passive vibration absorbers. Passive vibration absorbers are absorbed vibration without any control system and only reduce the system's vibration by absorbing energy and applying force at the proper frequency. The active vibration absorbers have similar benefits to passive vibration absorbers and have an active control system to reduce or control

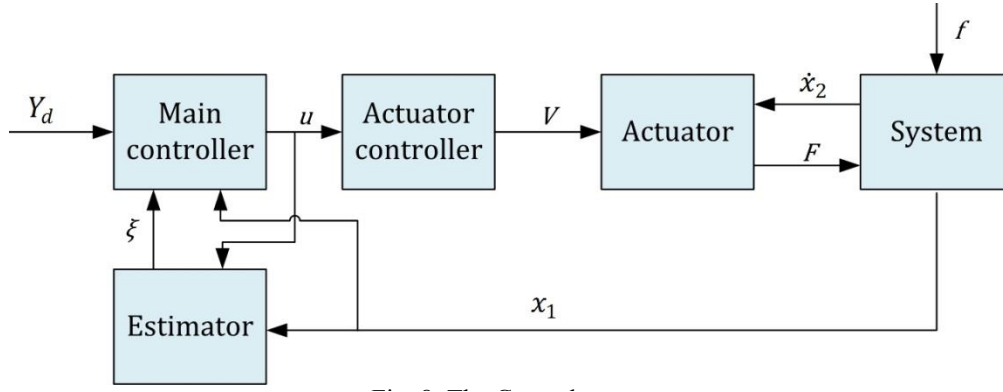


Fig. 8. The Control strategy

vibrations in different frequencies.

In the proposed control strategy, only the state-feedback of the main mass position  $x_1$  is used in the controller and the estimator. Fig. 8 shows the block diagram of the system with the controllers and the estimator. The output of the estimator is the value of the function  $\xi(t)$ . The magnetic actuator controller input is the output of the main controller, which is adjusted by the actuator voltage that indicates the force value of the actuator.

### 3- 2- 1- Feedback linearization controller

The error dynamics equation in the feedback linearization controller determines the behavior of the system. To this end, Eq. (28) is used for the error dynamics equation, a fourth-order differential equation.

$$e^{(4)} + a_3 e^{(3)} + a_2 \ddot{e} + a_1 \dot{e} + a_0 e = 0 \quad (28)$$

where  $a_0 \dots a_3$  are controller coefficients that can be determined concerning desired response and behavior. In Eq. (28), the error is defined as  $e = y_d - y$ . In fact, it is the error of the main mass position relative to the desired position. By substituting Eq. (22) into Eq. (28) and solving in terms of  $u$ , the feedback linearization controller is obtained as Eq. (29).

$$u = (v - \psi - \xi) \frac{m_1 m_2}{k_2} \quad (29)$$

where:

$$v = y_d^{(4)} - a_3 e^{(3)} - a_2 \ddot{e} - a_1 \dot{e} - a_0 e \quad (30)$$

$$\begin{aligned} \psi = & - \left( \frac{c_1}{m_1} + \frac{c_2}{m_2} \right) y^{(3)} - \\ & \left( \frac{k_1 + k_2}{m_1} + \frac{k_2}{m_2} + \frac{c_1 c_2}{m_1 m_2} \right) \ddot{y} - \\ & \left( \frac{c_1 k_2}{m_1 m_2} + \frac{c_2 (k_1 + k_2)}{m_1 m_2} \right) \dot{y} - \\ & \left( \frac{k_1 k_2}{m_1 m_2} \right) y - \left( \frac{k_2 k_{1p}}{m_1 m_2} \right) y^3 - \\ & \left( \frac{3k_{1p}}{m_1} \right) y^2 \ddot{y} - \left( \frac{6k_{1p}}{m_1} \right) y \dot{y}^2 - \left( \frac{3c_2 k_{1p}}{m_1 m_2} \right) y^2 \dot{y} \end{aligned} \quad (31)$$

Also,  $\xi$  is the estimated value by the estimator.

### 3- 2- 2- Sliding mode controller

The sliding mode controller is a robust control method used to compensate uncertainties and leads the system to the desired states. The sliding mode method is based on the Lyapunov stability theory [30]. Concerning Eq. (32), a sliding surface, according to Eq. (33), is considered. Based on this sliding surface, the sliding mode controller is designed for the system.

$$y^{(4)} = f(y) + \frac{k_2}{m_1 m_1} u(t) \quad (32)$$

$$s = e^{(3)} + 3\lambda \ddot{e} + 3\lambda^2 \dot{e} + \lambda^3 e \quad (33)$$

where  $s$  is sliding surface,  $\lambda$  is a constant which is defined such that  $p^3 + 3\lambda p^2 + 3\lambda^2 p + \lambda^3$  are stable (Hurwitz) polynomial and  $e = y_d - y$ .

The control goal of the sliding mode is defined so that the sliding surface converge to zero as follow:

$$s = 0 \rightarrow e^{(3)} + 3\lambda\ddot{e} + 3\lambda^2\dot{e} + \lambda^3e = 0 \quad (34)$$

To realize Eq. (34), the Lyapunov stability theory is used. To do this, the Lyapunov function is considered a definite positive function.

$$V = \frac{1}{2}s^2 > 0 \quad (35)$$

Now, for Eq. (34), the value  $u$  must be designed such that  $\dot{V}(s)$  be a negative definite.

$$\dot{V}(s) = s\dot{s} \quad (36)$$

The value of  $\dot{s}$  is obtained by differentiating from Eq. (33).

$$\dot{s} = y_d^{(4)} - y^{(4)} + 3\lambda e^{(3)} + 3\lambda^2\ddot{e} + \lambda^3\dot{e} \quad (37)$$

Substituting Eq. (32) into Eq. (37) leads to:

$$\dot{s} = y_d^{(4)} - f(y) - \frac{k_2}{m_1 m_2} u(t) + 3\lambda e^{(3)} + 3\lambda^2\ddot{e} + \lambda^3\dot{e} \quad (38)$$

To compensate for the uncertainty, the  $\dot{V}(s)$  is not only smaller than zero but its value is also considered smaller than a negative value as Eq. (39).

$$\dot{V}(s) = s\dot{s} \leq -\eta|s| \quad (39)$$

where  $\eta$  is a positive parameter. To find the equivalent controller, with regard to Eq. (38), the  $\dot{s}$  must be tended to zero, therefore by solving the resultant in terms of  $u$ , the equivalent controller is obtained as:

$$\dot{s} = 0 \rightarrow u_{eq} = \frac{m_1 m_2}{k_2} \times \left( y_d^{(4)} - f(y) + 3\lambda e^{(3)} + 3\lambda^2\ddot{e} + \lambda^3\dot{e} \right) \quad (40)$$

The controller is introduced by Eq. (40) is well if the system is completely known and accurate, but if there is uncertainty in the system, the values of  $f(y)$  are not completely known; so Eq. (40) rewrite based on the known value of  $f(y)$  denoted by  $\hat{f}(y)$  as the following form.

$$u_{eq} = \frac{m_1 m_2}{k_2} \times \left( y_d^{(4)} - \hat{f}(y) + 3\lambda e^{(3)} + 3\lambda^2\ddot{e} + \lambda^3\dot{e} \right) \quad (41)$$

To compensate for the uncertainties, the value of  $-k \operatorname{sgn}(s)$  is added to Eq. (40), and then the sliding mode controller is obtained as Eq. (42).

$$u = u_{eq} - k \operatorname{sgn}(s) \quad (42)$$

where  $k$  is a coefficient which is defined such that the  $\dot{V}$  be negative definite.

In the following, to prove the stability and to find the value of  $k$ , substituting Eq. (42) and Eq. (38) into the Eq. (39) as:

$$\begin{aligned} s\dot{s} &\leq -\eta|s| \xrightarrow{\frac{s}{|s|} = \operatorname{sgn}(s)} s \operatorname{sgn}(s) \leq -\eta \\ &\rightarrow (y_d^{(4)} - f(y) - \frac{k_2}{m_1 m_2} u(t) + 3\lambda e^{(3)} + 3\lambda^2\ddot{e} + \lambda^3\dot{e}) \operatorname{sgn}(s) \leq -\eta \\ &\rightarrow (y_d^{(4)} - f(y) - \frac{k_2}{m_1 m_2} (\frac{m_1 m_2}{k_2}) \times (y_d^{(4)} - \hat{f}(y) + 3\lambda e^{(3)} + 3\lambda^2\ddot{e} + \lambda^3\dot{e}) - k \operatorname{sgn}(s) + 3\lambda e^{(3)} + 3\lambda^2\ddot{e} + \lambda^3\dot{e}) \times \operatorname{sgn}(s) \leq -\eta \end{aligned} \quad (43)$$

In the sliding mode method, the uncertainty must be bounded, so:

$$|\hat{f}(y) - f(y)| \leq \rho \tag{44}$$

According to Eq. (43) and Eq. (44),  $k$  is obtained as follow:

$$\begin{aligned} \rho + \frac{k_2}{m_1 m_2} k &\leq -\eta \\ k &\leq -\frac{m_1 m_2}{k_2} (\eta + \rho) \end{aligned} \tag{45}$$

Finally, the sliding mode controller is rewritten in the form of Eq. (46).

$$\begin{aligned} u &= \frac{m_1 m_2}{k_2} \times \\ &\left( y_d^{(4)} - \hat{f}(y) + 3\lambda e^{(3)} + 3\lambda^2 \ddot{e} + \lambda^3 \dot{e} + (\eta + \rho) \text{sgn}(s) \right) \end{aligned} \tag{46}$$

### 3- 3- Magnetic actuator control

The magnetic actuator is modeled according to Eq. (9). Considering the very low self-inductance of the wire, as well as the low mutual inductance between the coils and the wire, Eq. (9) is rewritten as Eq. (47).

$$V_B = -R_e i - E \tag{47}$$

The force generated by the magnetic actuator is calculated in Eq. (18). By solving Eq. (18) in terms of  $V_B$ , the controller of the actuator is obtained as.

$$V_B = \frac{F_m R_e}{aB} + z_4 B a \tag{48}$$

By reducing the current of the coils, the density of the magnetic field is decreased. So we can neglect the effect of absorber speed. The controller of Eq. (48) cannot be implemented because there is no feedback from the absorber velocity  $z_4$ . Therefore, by reducing the current of coils, the effect of Faraday's induction is reduced, therefore the controller of Eq. (48) is approximated in the form of Eq. (49).

$$V_B = \frac{F_m R_e}{aB} \tag{49}$$

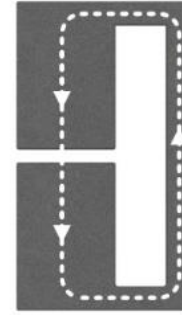


Fig. 9. The coil cross and path of magnetic flux

Because of the insignificant amount of inductance and the ignored effect of absorber velocity, the controller is actually a constant gain with the value  $R_e / aB$ . Another method to reduce inductance is related to the form of the coils winding. So, the distance between the wires must be very low and the wires must be wound together along with the core. Also, the magnetic core, as shown in Fig. 9, is designed as a closed-loop to minimize the loss of flux, which leads to decrease the mutual inductance.

### 4- Numerical Simulation

The performance of the mass-spring-damper system with vibration absorber and magnetic actuator with the controllers are simulated. The disturbance force is applied into the system as a sum of several sinusoidal forces with different frequencies, amplitude, and phase as

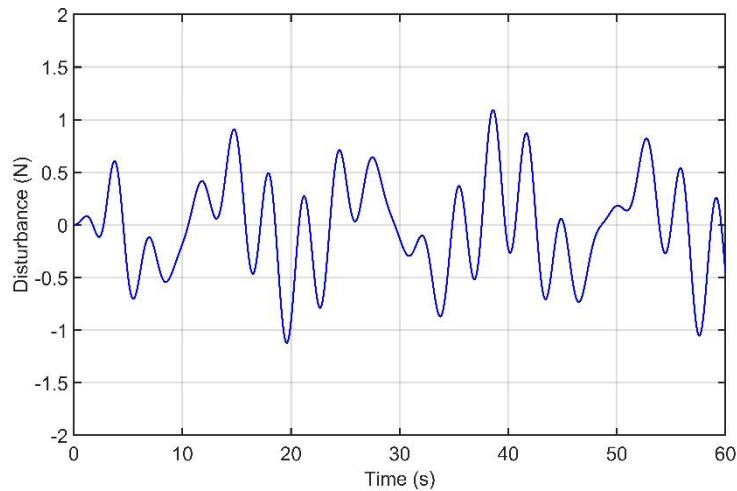
$$\begin{aligned} f &= 0.3 \sin\left(2.145t + \frac{\pi}{8}\right) + \\ &0.4 \sin\left(1.826t + \frac{\pi}{8}\right) + 0.45 \sin\left(0.49t + \frac{\pi}{3}\right) \end{aligned} \tag{50}$$

Fig. 10 shows the disturbance force, which is applied to the system.

The masses, springs, and dampers of the system are considered in Table 1. The absorber values are used based on Ref. [10].

By substituting the values of Table 1 in equations of the system and applying the disturbance force, the system's response with and without absorber is obtained. Fig. 11 shows the oscillations of the main system without an absorber, and Fig. 12 shows the oscillations of the main mass with the vibration absorber.

The controllers' effect can be observed by adding the magnetic actuator and controllers. Table 2 shows the parameters and coefficients of the magnetic actuator designed for the required control force.



**Fig. 10. The disturbance applied to the system**

**Table 1. The parameters and value of the primary system and absorber**

Parameters	Signs	Values
Primary mass	$m_1$	10 (kg)
Primary spring stiffness	$k_1$	44 (N/m)
Nonlinear primary spring stiffness	$k_{1p}$	8 (N/m <sup>3</sup> )
Primary damper	$c_1$	0.1 (Ns/m)
Absorber mass	$m_2$	0.6 (kg)
Absorber spring stiffness	$k_2$	2 (N/m)
Absorber damper	$c_2$	0.08 (Ns/m)

#### 4- 1- Estimator simulation results

The estimator helps to control the system by estimating a differential function of force disturbance  $\xi$ . The Liunberger observer estimates the value of  $\xi$ , and this value will be given for the controller to control the system. Fig. 13 shows the real value and estimated value of  $\xi$  with a step input.

According to Fig. 13, it can be seen that the estimated value is very close to the real value. In Fig. 13, the estimated value with the step input by using the feedback linearization controller. According to Fig. 13, when the input step is applied or accelerates movements, the estimation is accompanied by some quickly vanished errors.

#### 4- 2- Magnetic actuator controller

The magnetic actuator controller is obtained by eliminating the velocity of the absorber mass in the controller of the magnetic actuator and minimizing the effect of the inductance in this system. The magnetic actuator controller has an appropriate response to the desired force which is determined by the main controller. Fig. 14 shows the desired force determined by the feedback linearization controller and the output force of the actuator which is controlled by means of the magnetic actuator controller.

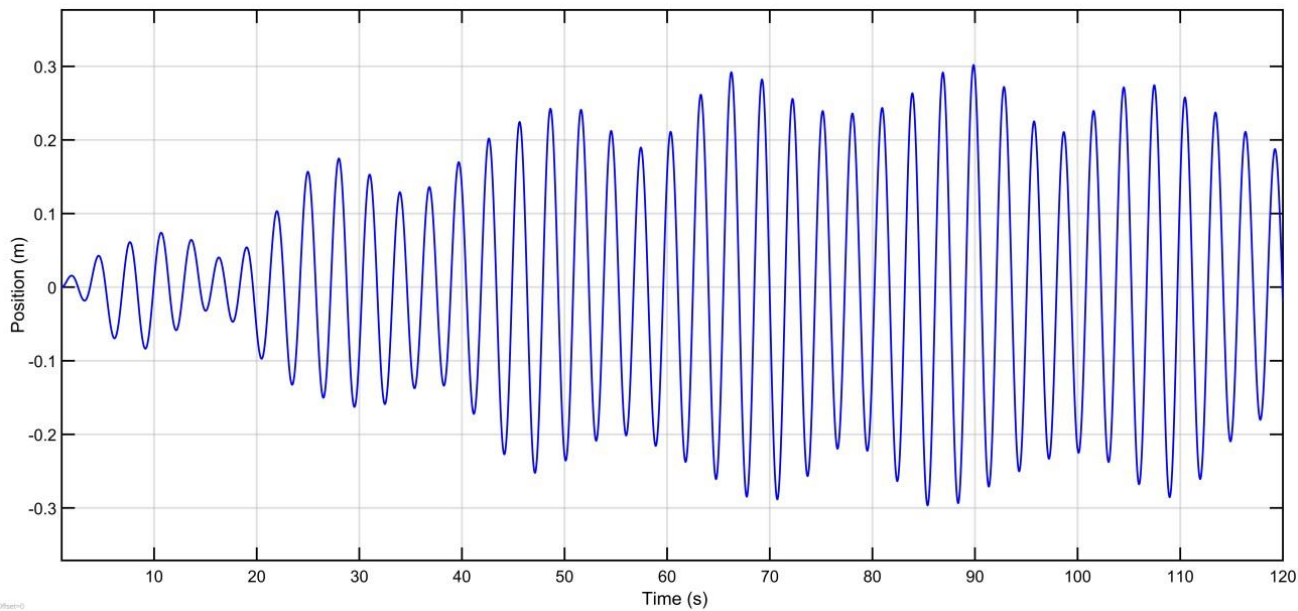


**Fig. 11. Oscillations of the primary system without absorber**

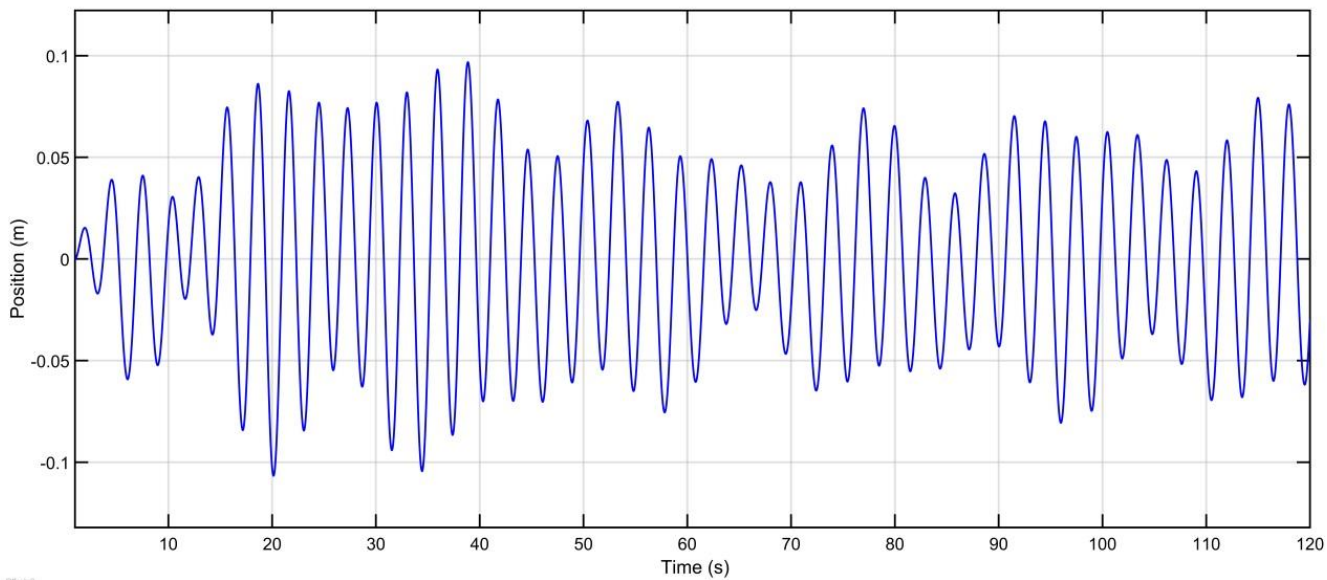


**Fig. 12. Oscillations of the primary system with passive vibration absorber**

**Table 2. Parameters and value of the magnetic actuator**

Parameters	Signs	Values
Number of rings	$N$	50
Vacuum permittivity	$\mu_0$	$4\pi * 10^{-7}$ (H/m)
The relative permittivity of Iron	$\mu_r$	4000
Current of coils	$I_f$	0.5 (A)
Width of coils	$a$	0.04 (m)
Length of coils	$b$	0.5 (m)
Resistance of coil	$R$	2 ( $\Omega$ )

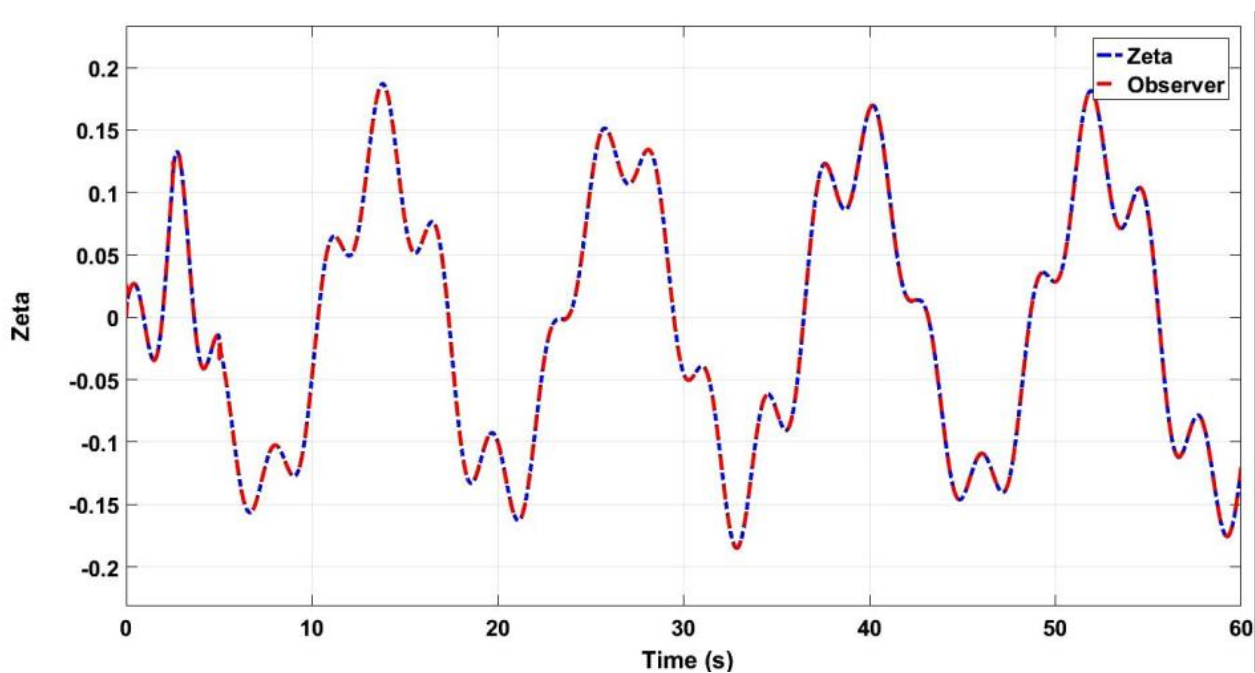


**Fig. 13. Estimation of  $\xi$**

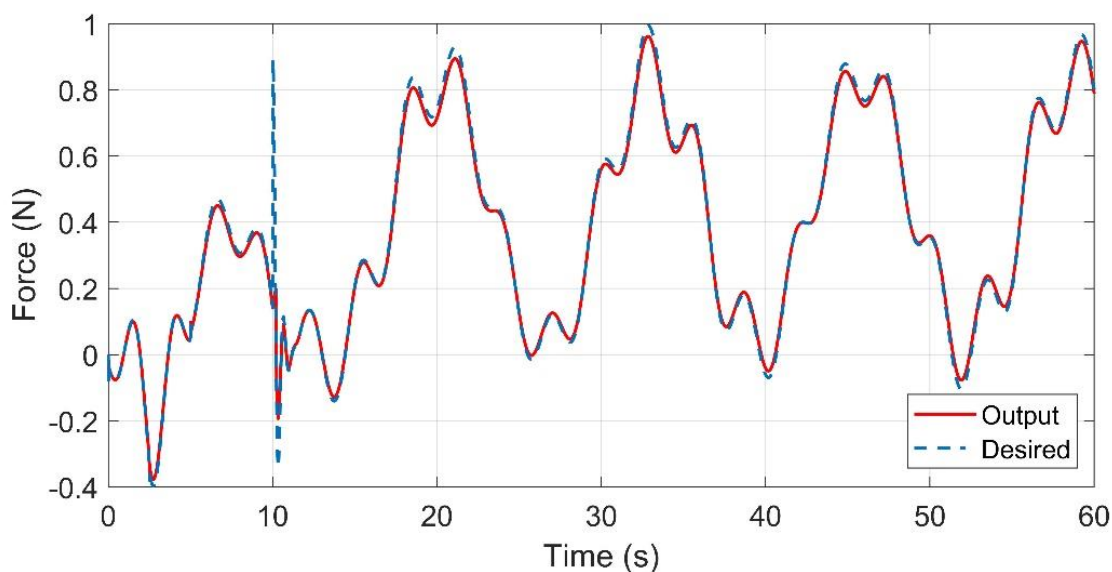


**Fig. 14. The actuator and its controller response to the main controller**

## 5- Optimization

### 5- 1- Metaheuristic techniques

Metaheuristic techniques usually mimic natural, physical or cultural events for solving optimization problems. These methods can be categorized into four classes: swarm-based, evolution-based, human-based, and physics-based techniques [34]. The most popular techniques in these classifications are shown in Fig. 15. Evolutionary optimization algorithms are developed by the rules of natural evolution. The most popular evolution-based algorithm inspired by Darwinian evolution is Genetic Algorithms (GA) [35], where it is used in many optimization problems. The other group, where simulate the social behavior of groups of birds, animals, and so on, is called swarm-based algorithms. Particle Swarm Optimization (PSO), where mimics the bird's flock's group relations, is the most famous method in swarm-based optimization algorithms [36].

Moreover, Physics-based methods simulate physical events in nature. The most popular method in this category is Simulated Annealing (SA) [37], based on the annealing process in material science. In the last category, there are some metaheuristic techniques motivated by human and social behaviors.

In the current study, four techniques, namely, GA, PSO, SA, and Teach-Learn-Based Optimization (TLBO), are considered to optimize the optimization problems. It should be noted that these algorithms were chosen in different groups.

### 5- 2- Optimizing of the controller coefficients

The controller coefficients in the feedback linearization method and the sliding mode method are usually obtained by

simulation trial and error. In this approach, the coefficients of the feedback linearization controllers, including  $a_0, a_1, a_2, a_3$ , and sliding mode, including  $\lambda$  is obtained by optimization, is optimized by different metaheuristic algorithms. Settling time is minimized by calculating these coefficients by algorithms. To obtain the controllers' best coefficients, the cost function and the constraints must be defined for optimization. The settling time is defined as a cost function and the error is defined as constraints. The step input is considered the desired input for the system; when the error is lower than 0.5% of step input, and the speed, acceleration, and jerk of the system tend to zero, the settling time is obtained. Each algorithm is run ten times with different coefficient values, and the coefficients related to the best run have been selected and are shown in Table 3. Ranges of the design variables for all algorithms are selected as  $a_0 = [0, 1000]$ ,  $a_1 = [0, 1000]$ ,  $a_2 = [0, 200]$ ,  $a_3 = [0, 100]$  and  $\lambda = [0, 100]$ . Table 3 shows the value of population, iteration, and probable coefficients for different algorithms.

Fig. 16 shows that the optimization algorithm reduces the system response's settling time with the feedback linearization controller.

Fig. 17 shows each algorithm's best outputs for the feedback linearization controller and the effect of changing the coefficients in which PSO has the best result.

The optimization of the sliding mode controller coefficient is similar to the feedback linearization coefficients optimization. Fig. 18 shows the reduction of the settling time, and Fig. 19 shows the best output of each algorithm.

Comparisons of four optimization algorithms are represented in Tables 4 and 5. PSO algorithm has the best result for the feedback linearization coefficient in the Table 4.

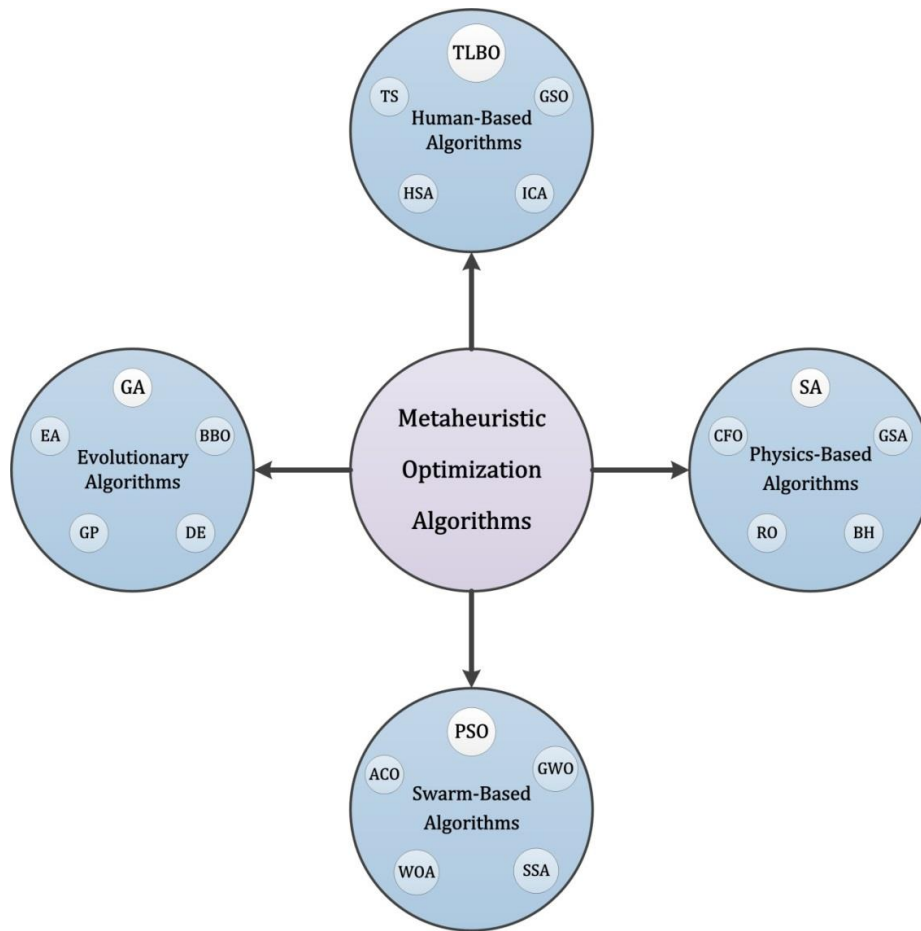


Fig. 15. Classification of the metaheuristic techniques

Table 3. The best-used optimization techniques parameters

Parameter	Controller	GA	PSO	SA	TLBO
Maximum Number of Iterations	F-L	100	100	100	100
	SMC	40	40	40	40
Initial Population Size	F-L	100	100	100	100
	SMC	10	10	10	10
Crossover Coefficient	F-L	0.9	-	-	-
	SMC	0.9	-	-	-
Mutation Coefficient	F-L	0.1	-	-	-
	SMC	0.1	-	-	-
Inertia Term	F-L	-	0.7	-	-
	SMC	-	0.3	-	-

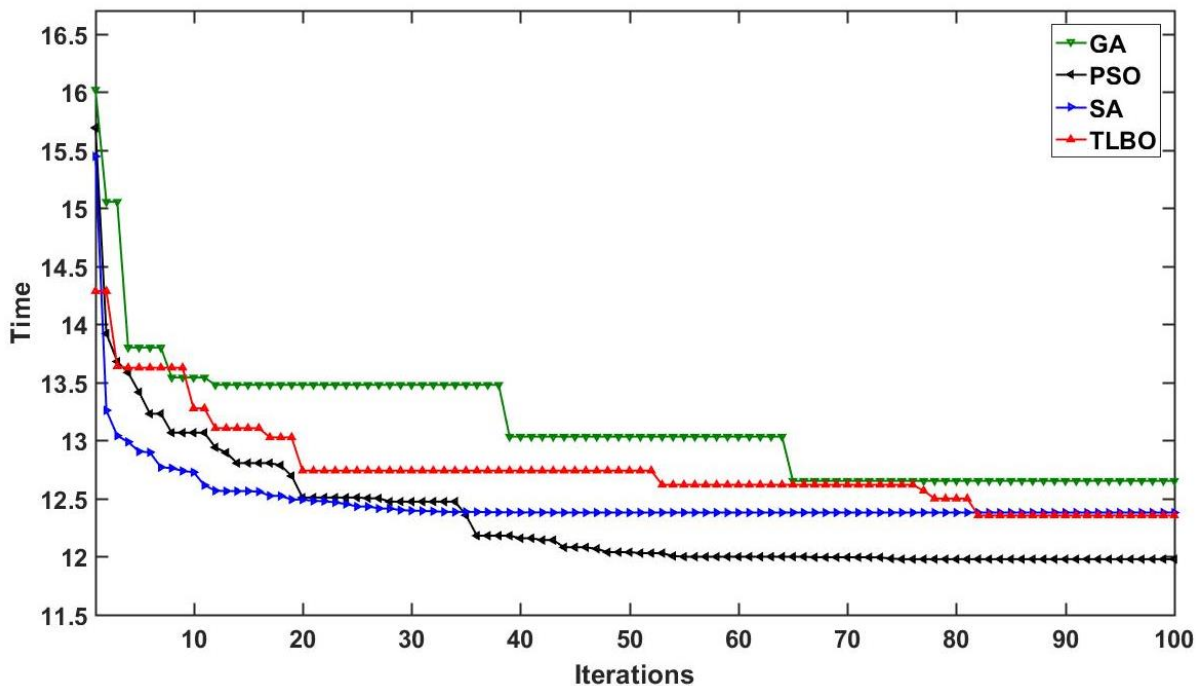


Fig. 16. Decreasing the settling time with optimization algorithms for the feedback linearization controller

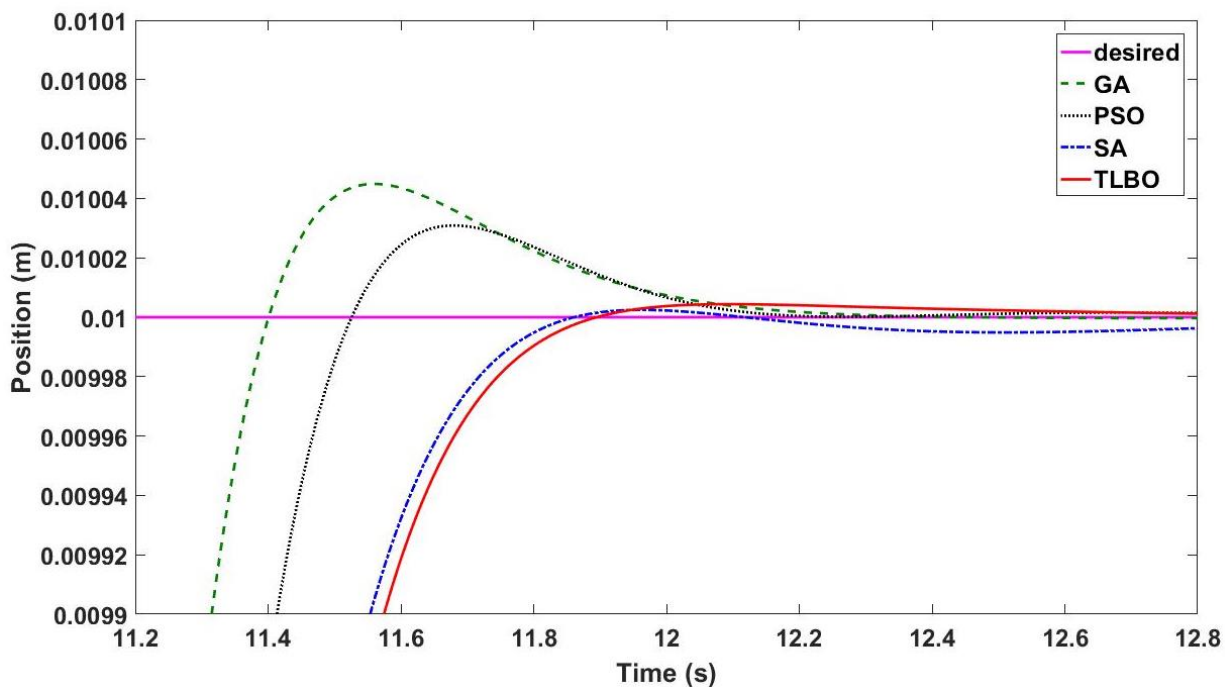


Fig. 17. The optimizing settling time for the step input in case of feedback linearization controller

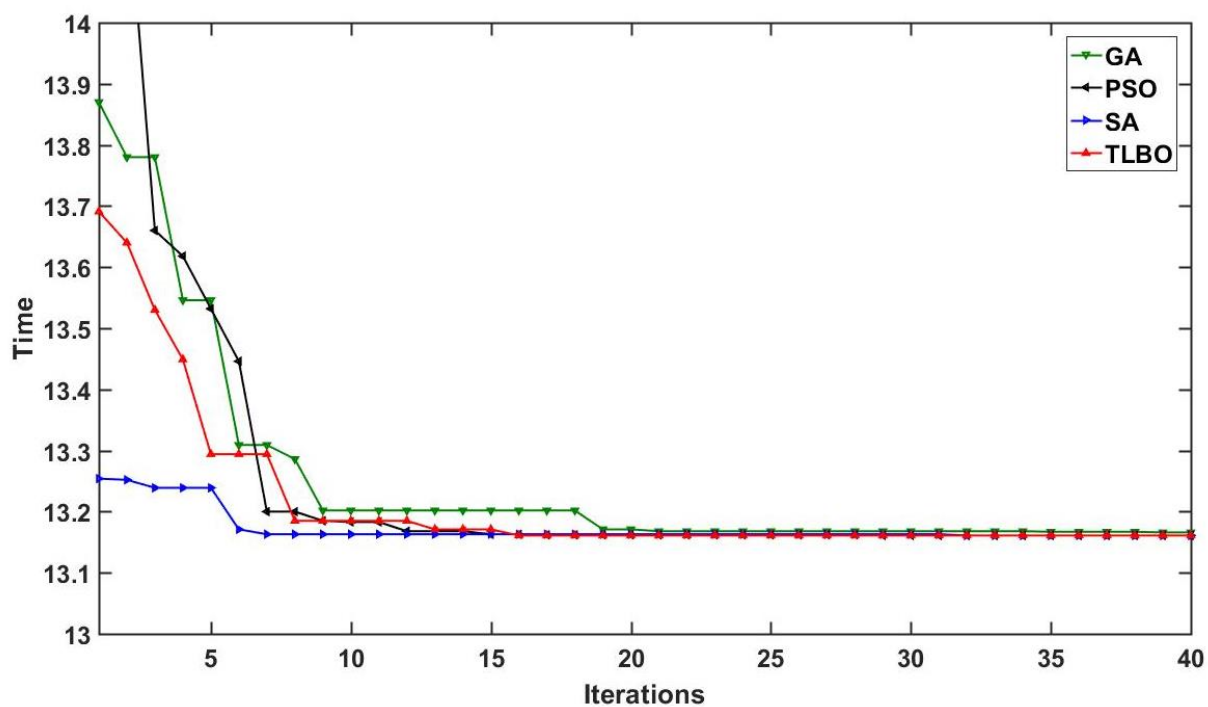


Fig. 18. Decreasing the settling time with optimization algorithms for the sliding mode controller

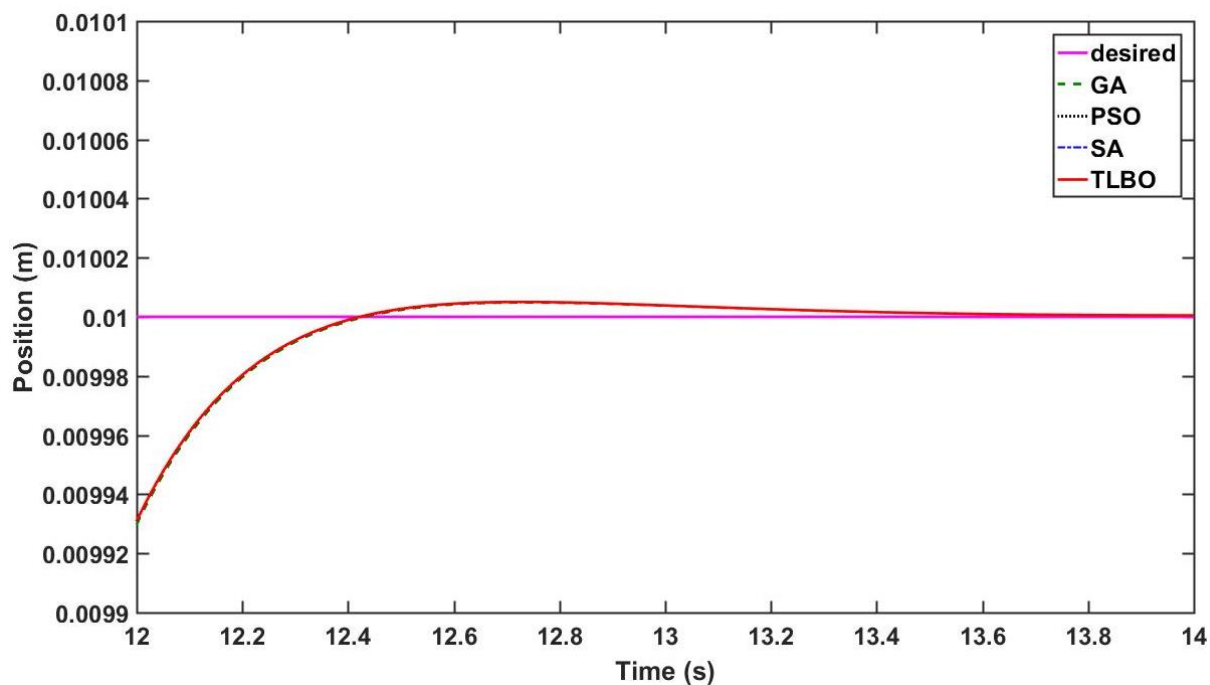
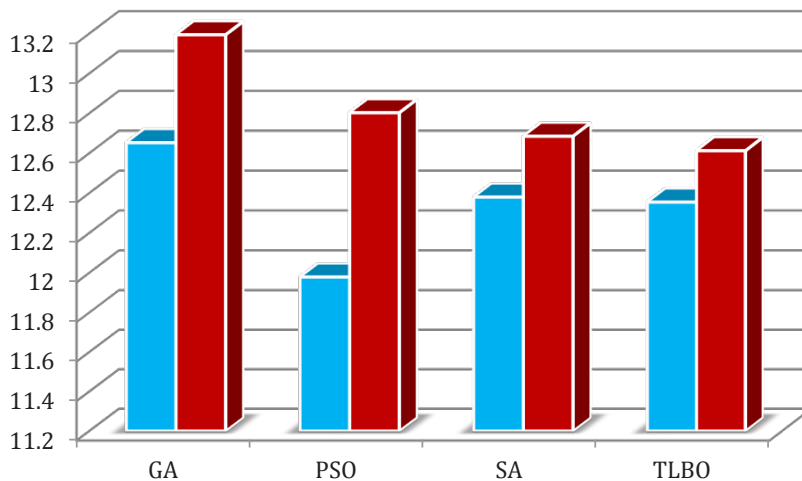


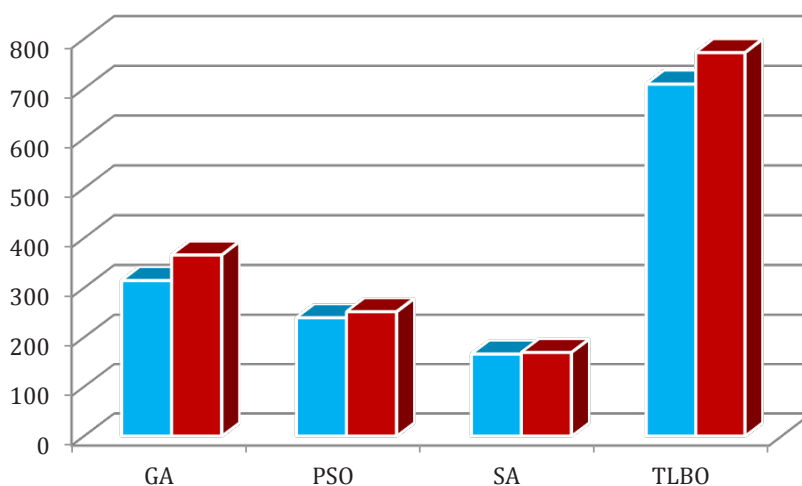
Fig. 19. The optimizing settling time for the step input in case of the sliding mode controller

**Table 4. Comparing results of optimization algorithms for feedback linearization coefficients**

Algorithm	Optimal Design variables				Cost Function		CPU Time (s)	
	$a_0$	$a_1$	$a_2$	$a_3$	Best (s)	Average (s)	Best (s)	Average (s)
GA	739.1176	487.3704	138.9523	18.0493	12.653	13.1943	314.1329	365.4614
PSO	563.9815	390.7921	109.9931	15.394	11.979	12.8033	239.3058	251.494
SA	1000	704.7331	196.87	25.178	12.38	12.6854	165.7098	169.0135
TLBO	579.6328	414.7801	118.5773	16.3557	12.355	12.6123	708.8619	772.0213



a) Cost Function ( Best (s) Average (s))

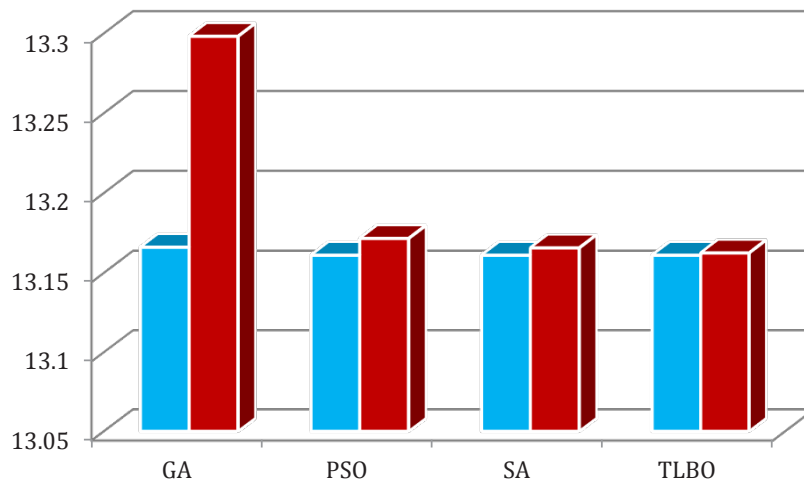


b) CPU time ( Best (s) Average (s))

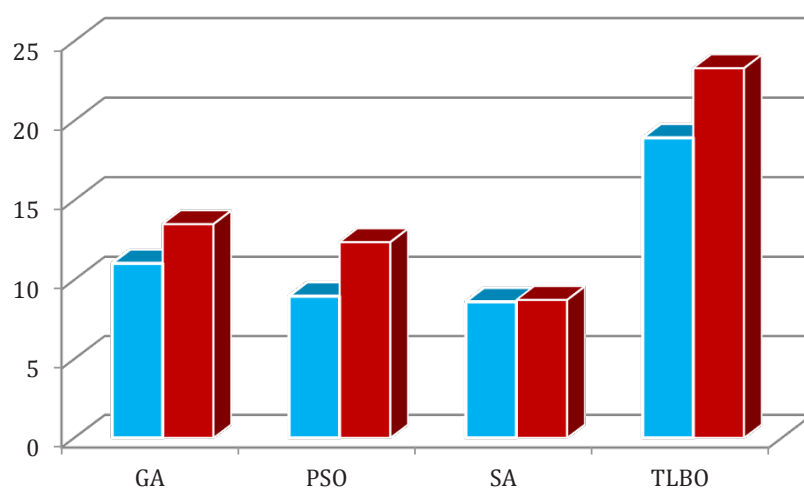
**Fig. 20. Comparison of the optimization algorithms for feedback linearization coefficients**

**Table 5. Comparing results of optimization algorithms for sliding mode coefficient**

Algorithm	Optimal Design variables	Cost Function		CPU Time (s)	
	$\lambda$	Best (s)	Average (s)	Best (s)	Average (s)
GA	4.6912	13.166	13.2981	11.0297	13.493
PSO	4.6964	13.161	13.1715	8.9656	12.3612
SA	4.6964	13.161	13.1656	8.615	8.7320
TLBO	4.6964	13.161	13.1624	18.9172	23.2915



a) Cost Function ( ■ Best (s) ■ Average (s))



b) CPU time ( ■ Best (s) ■ Average (s))

**Fig. 21. Comparison of the optimization algorithms for sliding mode coefficient**

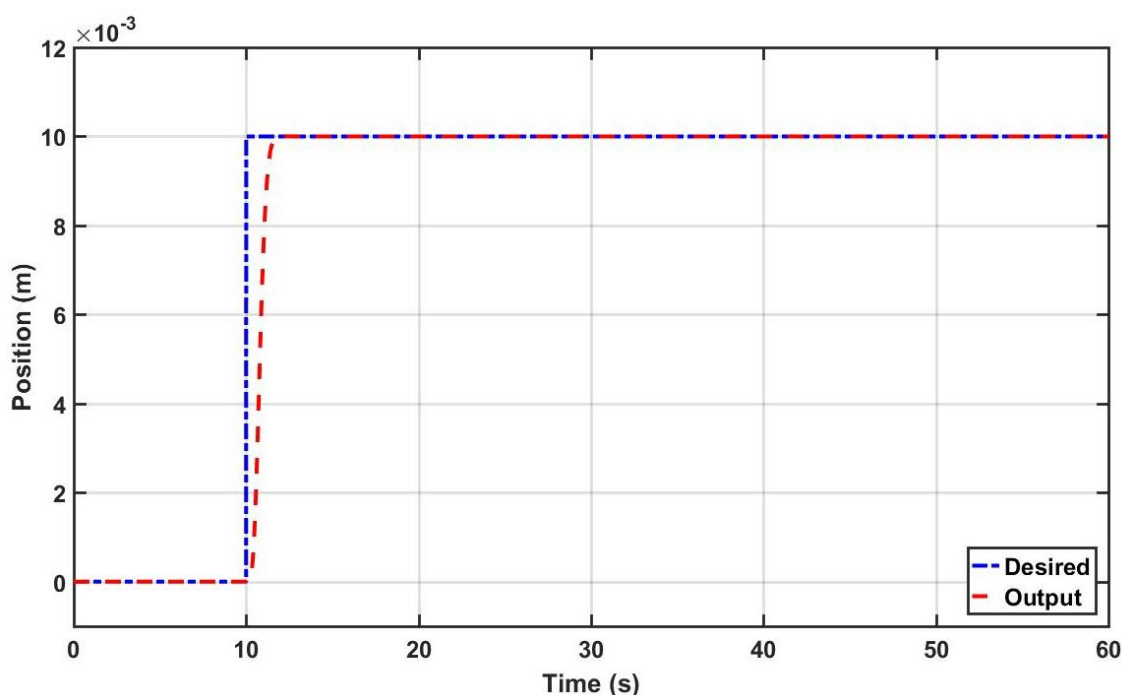


Fig. 22. The system response in case of feedback linearization controller without uncertainty

TLBO has not tuned parameter and has the Best average. It means that the PSO tuning parameter must be select correctly. By comparing the best results and averages, if a suitable tuning parameter selects for PSO, it has the best result else TLBO is a good choice for this system and feedback linearization controller. According to the CPU time in Tables 4 and 5, SA. is the fastest, and TLBO is the slowest among four different algorithms.

## 6- Results

Feedback linearization and sliding mode control are simulated for two situations: system uncertainty and system uncertainty. If uncertainty exists in the system, the estimation error is increased because the estimator is based on the system's model.

### 6- 1- Control simulation (without system uncertainty and with force uncertainty)

The feedback linearization strategy controls the main mass's position by applying the control force on the absorber mass. Fig. 22 shows the system response in the case of a feedback linearization controller due to the step input. The feedback linearization coefficients values are derived from the PSO algorithm as  $a_0=563.98$ ,  $a_1=390.79$ ,  $a_2=109.99$  and  $a_3=15.39$ .

Fig. 23 shows the sliding mode response to a step input. It can be seen, sliding mode controller without uncertainty is provided an appropriate response. The value of  $\lambda$  in this

control method is 4.6964, which is obtained from optimization algorithms.

### 6- 2- Control Simulation (with system and force uncertainty)

The feedback linearization controller is not provided a proper response in the presence of parametric uncertainty. Fig. 24 shows the system response by using the feedback linearization controller, including the uncertainty.

Fig. 25 shows the system response with a sliding mode controller in uncertainty, which has a suitable response.

## 7- Conclusions

An active vibration absorber was utilized in this study for a nonlinear one degree of freedom system with an unknown multi-harmonic frequency disturbance force. A function of disturbance was estimated by the Liunberger observer. Then the system was controlled by feedback linearization and sliding mode controllers. Finally, the settling time was optimized by GA, PSO, SA, and TLBO algorithms. Some results in this study are summarized as follows:

In the absence of uncertainty, feedback linearization is faster than the sliding mode controller.

In the presence of uncertainty, the feedback linearization has the error, but this error is lower when its coefficients are optimal.

In the presence of uncertainty, the sliding mode is slower than the case without uncertainty.

The optimization of controller coefficients to reduce the

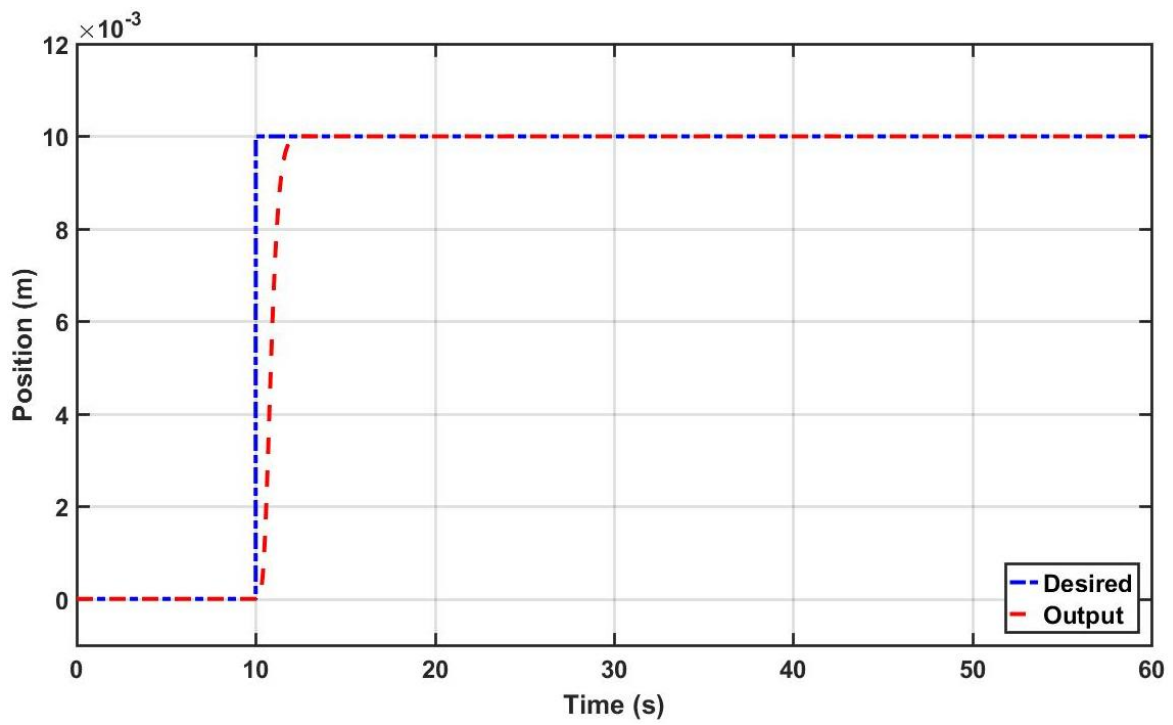


Fig. 23. The system response in case of sliding mode controller without uncertainty

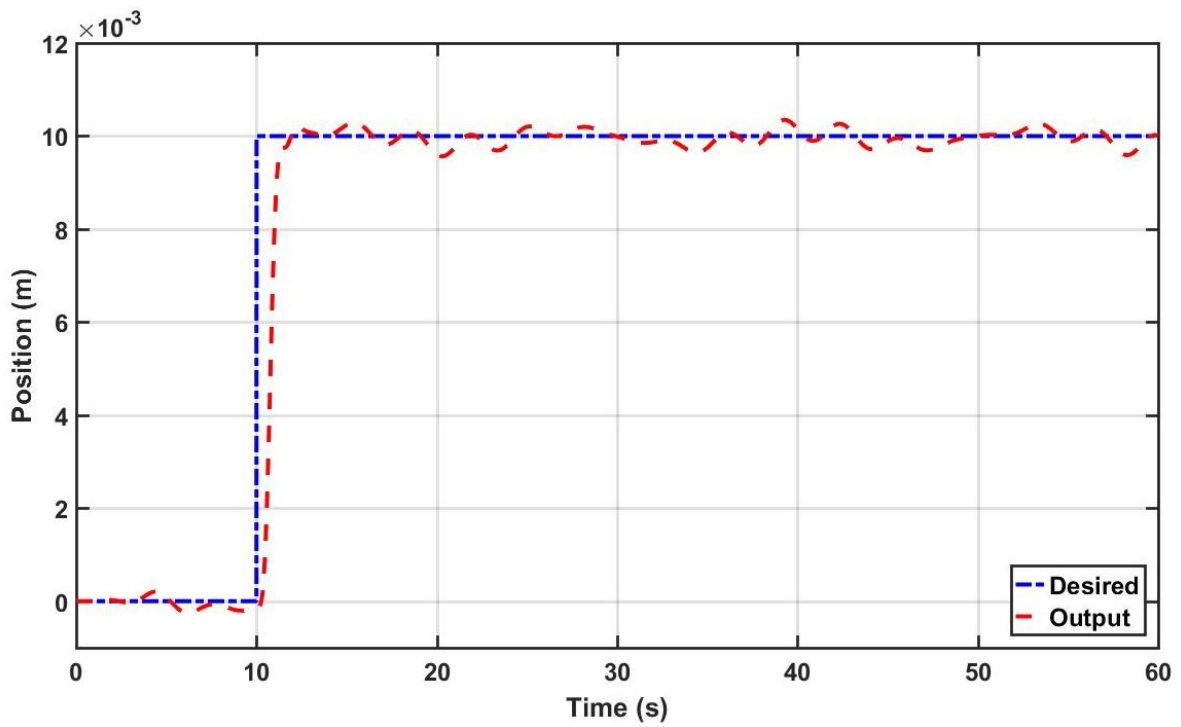
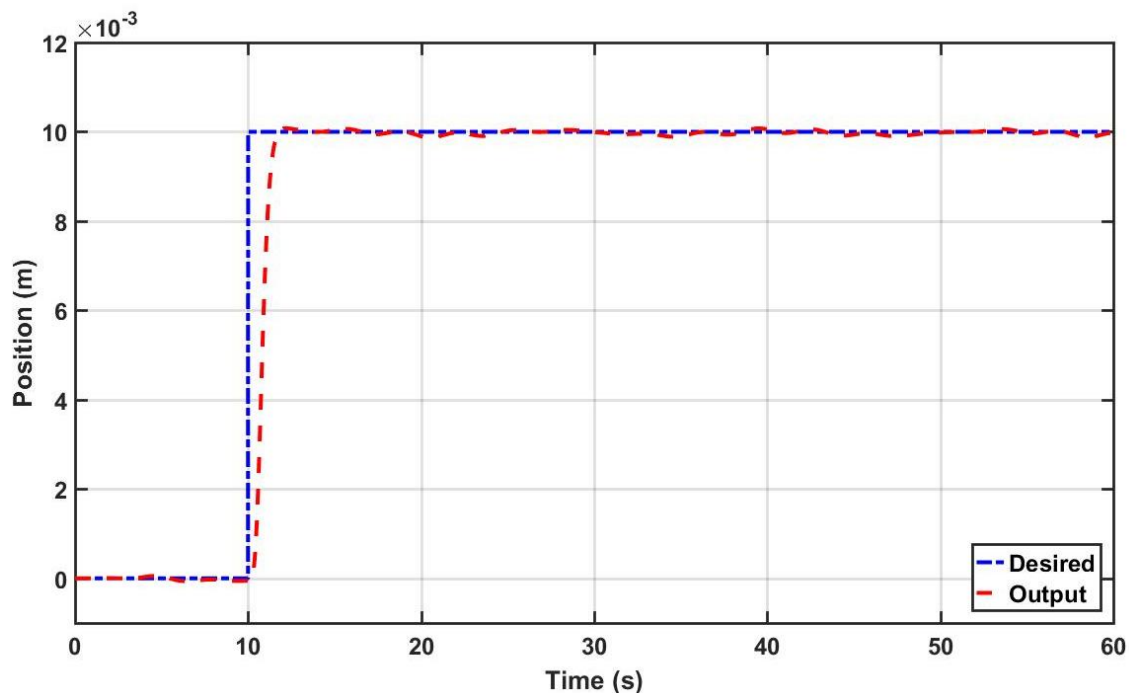


Fig. 24. The system response in case of feedback linearization controller with uncertainty



**Fig. 25. The system response in case of sliding mode controller with uncertainty.**

settling time increases the speed and accuracy of the system response

Comparing four different optimization algorithms for our problem shows that PSO, as a swarm-based algorithm, has the best response.

Moreover, TLBO, as a human-based algorithm, is more confident because its average is better than the others.

Furthermore, the SA, as a physics-based algorithm, is the fastest method for calculating the controller coefficient.

## References

- [1] P. Bonello, Adaptive tuned vibration absorbers: Design principles, concepts and physical implementation, in: *Vibration Analysis and Control-New Trends and Developments*, InTech, 2011.
- [2] E. Caetano, Á. Cunha, C. Moutinho, F. Magalhães, Studies for controlling human-induced vibration of the Pedro e Inês footbridge, Portugal. Part 2: Implementation of tuned mass dampers, *Engineering Structures*, 32(4) (2010) 1082-1091.
- [3] A.H. Nayfeh, D.T. Mook, *Nonlinear oscillations*, John Wiley & Sons, 2008.
- [4] T. Taniguchi, A. Der Kiureghian, M. Melkumyan, Effect of tuned mass damper on displacement demand of base-isolated structures, *Engineering Structures*, 30(12) (2008) 3478-3488.
- [5] J. Ji, N. Zhang, Suppression of the primary resonance vibrations of a forced nonlinear system using a dynamic vibration absorber, *Journal of Sound and Vibration*, 329(11) (2010) 2044-2056.
- [6] X. Chen, A. Kareem, Efficacy of tuned mass dampers for bridge flutter control, *Journal of Structural Engineering*, 129(10) (2003) 1291-1300.
- [7] A. Baz, A neural observer for dynamic systems, *Journal of sound and vibration*, 152(2) (1992) 227-243.
- [8] J.-S. Bae, J.-H. Hwang, J.-H. Roh, J.-H. Kim, M.-S. Yi, J.H. Lim, Vibration suppression of a cantilever beam using magnetically tuned-mass-damper, *Journal of Sound and Vibration*, 331(26) (2012) 5669-5684.
- [9] E. El Behady, E. El-Zahar, Vibration reduction and stability study of a dynamical system under multi-excitation forces via active absorber, *International Journal of Physical Sciences*, 7(48) (2013) 6203-6209.
- [10] F. Beltran-Carbajal, G. Silva-Navarro, Active vibration control in Duffing mechanical systems using dynamic vibration absorbers, *Journal of sound and vibration*, 333(14) (2014) 3019-3030.
- [11] T. Bailey, J.E. Hubbard, Distributed piezoelectric-polymer active vibration control of a cantilever beam, *Journal of Guidance, Control, and Dynamics*, 8(5) (1985) 605-611.
- [12] R. Zhang, C. Tong, Torsional vibration control of the main drive system of a rolling mill based on an extended state observer and linear quadratic control, *Journal of Vibration and Control*, 12(3) (2006) 313-327.
- [13] F. Beltrán-Carbajal, G. Silva-Navarro, Adaptive Like Vibration Control in Mechanical Systems with Unknown Parameters and Signals, *Asian Journal of Control*, 15(6) (2013) 1613-1626.

- [14] N. Al-Holou, T. Lahdhiri, D.S. Joo, J. Weaver, F. Al-Abbas, Sliding mode neural network inference fuzzy logic control for active suspension systems, *IEEE Transactions on Fuzzy Systems*, 10(2) (2002) 234-246.
- [15] Z. Xianmin, S. Changjian, A.G. Erdman, Active vibration controller design and comparison study of flexible linkage mechanism systems, *Mechanism and Machine Theory*, 37(9) (2002) 985-997.
- [16] S.-B. Choi, Y.-M. Han, Vibration control of electrorheological seat suspension with human-body model using sliding mode control, *Journal of Sound and Vibration*, 303(1-2) (2007) 391-404.
- [17] C. Hansen, S. Snyder, X. Qiu, L. Brooks, D. Moreau, *Active control of noise and vibration*, CRC press, 2012.
- [18] M. McLaren, G. Slater, A disturbance model for control/structure optimization with output feedback control, *Structural optimization*, 6(2) (1993) 123-133.
- [19] G. Zhao, B. Chen, Y. Gu, Control-structural design optimization for vibration of piezoelectric intelligent truss structures, *Structural and Multidisciplinary Optimization*, 37(5) (2009) 509.
- [20] X. Zhang, A. Takezawa, Z. Kang, Topology optimization of piezoelectric smart structures for minimum energy consumption under active control, *Structural and Multidisciplinary Optimization*, 58(1) (2018) 185-199.
- [21] P. Bisegna, G. Caruso, Optimization of a passive vibration control scheme acting on a bladed rotor using an homogenized model, *Structural and Multidisciplinary Optimization*, 39(6) (2009) 625.
- [22] E. Boroson, S. Missoum, Stochastic optimization of nonlinear energy sinks, *Structural and Multidisciplinary Optimization*, 55(2) (2017) 633-646.
- [23] I. Venanzi, Robust optimal design of tuned mass dampers for tall buildings with uncertain parameters, *Structural and Multidisciplinary Optimization*, 51(1) (2015) 239-250.
- [24] D. Howe, Magnetic actuators, *Sensors and Actuators A: Physical*, 81(1-3) (2000) 268-274.
- [25] S.-M. Jang, J.-Y. Choi, S.-H. Lee, H.-W. Cho, W.-B. Jang, Analysis and experimental verification of moving-magnet linear actuator with cylindrical Halbach array, *IEEE transactions on magnetics*, 40(4) (2004) 2068-2070.
- [26] N. Mikhaeil-Boules, Design and analysis of linear actuator for active vibration cancellation, in: *Industry Applications Conference, 1995. Thirtieth IAS Annual Meeting, IAS'95, Conference Record of the 1995 IEEE, IEEE, 1995*, pp. 469-475.
- [27] S. Evans, I. Smith, J. Kettleborough, Permanent-magnet linear actuator for static and reciprocating short-stroke electromechanical systems, *IEEE/ASME transactions on mechatronics*, 6(1) (2001) 36-42.
- [28] Q. Li, F. Ding, C. Wang, Novel bidirectional linear actuator for electrohydraulic valves, *IEEE transactions on magnetics*, 41(6) (2005) 2199-2201.
- [29] J. Kim, J. Chang, A new electromagnetic linear actuator for quick latching, *IEEE Transactions on Magnetics*, 43(4) (2007) 1849-1852.
- [30] A.E. Rundell, S.V. Drakunov, R.A. DeCarlo, A sliding mode observer and controller for stabilization of rotational motion of a vertical shaft magnetic bearing, *IEEE Transactions on Control Systems Technology*, 4(5) (1996) 598-608.
- [31] C. Van Lierop, J. Jansen, A. Damen, E. Lomonova, P. Van den Bosch, A. Vandenput, Model-based commutation of a long-stroke magnetically levitated linear actuator, *IEEE Transactions on Industry Applications*, 45(6) (2009) 1982-1990.
- [32] H. Guckel, T. Earles, J. Klein, J. Zook, T. Ohnstein, Electromagnetic linear actuators with inductive position sensing, *Sensors and Actuators A: Physical*, 53(1-3) (1996) 386-391.
- [33] DK. Cheng, *Field and wave electromagnetics*, Pearson Education India, 1989.
- [34] S. Mirjalili, A. Lewis, The whale optimization algorithm, *Advances in engineering software*, 95 (2016) 51-67.
- [35] S. Sivanandam, S. Deepa, *Genetic algorithms, in: Introduction to genetic algorithms*, Springer, 2008, pp. 15-37.
- [36] J. Kennedy, R. Eberhart, Particle swarm optimization, in: *Proceedings of ICNN'95-international conference on neural networks, IEEE, 1995*, pp. 1942-1948.
- [37] M. Pincus, Letter to the editor—a monte carlo method for the approximate solution of certain types of constrained optimization problems, *Operations research*, 18(6) (1970) 1225-1228.

#### HOW TO CITE THIS ARTICLE

M. AbdolMohammadi, H. Ahmadi, S. M. Varedi-Koulaei, J. Ghalibafan, *Active Vibration Control of a Nonlinear System with Optimizing The Controller Coefficients Using Metaheuristic Algorithms*, *AUT J. Mech Eng.*, 5(4) (2021) 511-534.

DOI: [10.22060/ajme.2021.19740.5962](https://doi.org/10.22060/ajme.2021.19740.5962)



